OE Optical Engineering

RESEARCH PAPER

Optimal design and preparation of high-performance multilayered thin film daytime radiative coolers

Yu-Shan Zhang,[a] Bao-Jian Liu,[a,b] Xiao-Jie Sun,[a] Wei-Bo Duan,[b,*] Yu-Ting Yang,[a] De-Ming Yu,[b] Qing-Yuan Cai,[b] Hao-Tian Zhang,[a] Lei Peng,[a] Rong-Jun Zhang,[a] and Yu-Xiang Zheng[a,c,*]

[a]Ministry of Education, Fudan University, School of Information Science and Engineering, Shanghai Engineering Research Center of Ultra-Precision Optical Manufacturing, Key Laboratory of Micro and Nano Photonic Structures, Shanghai, China
[b]Chinese Academy of Sciences, Shanghai Institute of Technical Physics, Shanghai Key Laboratory of Optical Coatings and Spectral Modulation, Shanghai, China
[c]Fudan University, Yiwu Research Institute of Fudan University, Zhejiang, China

ABSTRACT. Radiative cooling is a passive cooling strategy that can radiate heat to outer space through the 8 to 13 μm waveband (atmospheric window) and is now widely used for buildings, wearable fabric, solar cells, and electronic devices. Daytime radiative cooling requires both high reflection in the solar spectrum and high absorption/emission in the 8 to 13 μm range. Previous multilayered structures were optimized by changing the thickness ratio of the layers, but the optical properties of multilayer thin films, such as absorptivity, transmissivity, and reflectivity, are determined by complex factors. In this work, several initial multilayer structures were selected and then the thickness of each layer was globally optimized; the theoretically smallest thickness with the best absorption performance was achieved in the 8 to 13 μm range, which significantly improved the cooling performance and reduced costs. We developed an optimized SiO_2-Ta_2O_5 alternating multilayer photonic radiative cooling thin film and fabricated it using ion source assisted electron beam evaporation with an average emissivity of 0.876 within the 8 to 13 μm range and an average reflectivity of 0.963 in the 0.3 to 2.5 μm waveband; it achieved an average temperature reduction of 20.1°C lower than the uncoated substrate and 3.2°C lower than the ambient temperature under direct sunlight with an average solar power of 859.3 W/m^2.

Keywords: radiative cooling; thin film; ideal emissive spectrum; design; optimization

Paper 20240121SS received Jan. 31, 2024; revised May 12, 2024; accepted Jun. 5, 2024; published Jul. 9, 2024.

1 Introduction

With global warming and increasing usage of various kinds of electric apparatuses, the world has a growing demand for cooling.[1–8] Traditional cooling modes are air cooling, water cooling, etc., through the process of heat conduction and convection to take away the heat in the device. However, this cooling method requires additional energy consumption and increases the complexity of the system, thus reducing the reliability. Radiative cooling[9–15] has attracted public attention as a passive cooling method without any energy input or greenhouse gas emissions.

*Address all correspondence to Wei-Bo Duan, duanweibo@mail.sitp.ac.cn; Yu-Xiang Zheng, yxzheng@fudan.edu.cn

During the process of radiative cooling, heat can be automatically transferred from an object at ambient temperature on Earth to space with a temperature of only 3 K through the 8 to 13 μm waveband, known as the atmospheric window.[16–18]

Multilayer film structures have been widely used in filter films, antireflection films, broadband absorption films, and other applications. In the last decade, their applications in radiative cooling have also received attention.[19–24] Daytime radiative cooling, which requires not only high emission in the atmospheric window waveband but also high reflection in the solar spectrum, is quite difficult to design in two wide wavebands. Fan's group[19] first achieved a multilayered daytime radiative cooling thin film using an HfO_2-SiO_2 alternating structure, which had an average reflectivity of 97% in the 0.3 to 2.5 μm waveband and an average absorptivity of 67% within the 8 to 13 μm waveband. It reached an average temperature reduction of 4.9°C. Kecebas et al.[20] designed and fabricated a radiative cooler by applying a multilayer structure using SiO_2, TiO_2, and Al_2O_3. It achieved an average absorptivity of 78% within the 8 to 13 μm range. Jeong et al.[21] developed a photonic radiative cooler with an average absorptivity of 84% in the atmospheric window. Its structure showed a better performance in nighttime radiative cooling than the HfO_2-SiO_2 cooler. However, the high absorption of TiO_2 in the near ultraviolet band makes it not as good as the HfO_2-SiO_2 cooler in solar reflection, and the total thickness of 4 μm increases the risk of film cracking or delamination. Recently, Xiao et al.[24] chose 18 alternating layers of three materials, SiN, SiO_2, and Ta_2O_5, on top of an Al mirror back reflector, with a total thickness of only 2.088 μm. They accomplished an average reflectivity of over 89% of the incident solar power from 0.3 to 2.5 μm and an average thermal infrared absorptivity of 75% in the 2.5 to 30 μm range.

Previous studies have shown that stacking different types of dielectric layers enables a daytime radiative cooler with as high performance by changing the thickness and material of each layer. This study introduces the optimal design and preparation of a multilayered photonic radiative cooler. We conduct a comprehensive analysis of various oxides and metals, ultimately choosing SiO_2, Ta_2O_5, Al_2O_3, and Ag for the initial structure. Subsequently, global optimization is performed to achieve optimal performance while minimizing the thickness, aiming for the thinnest possible configuration with the highest efficiency. On the basis of the designed structures, we fabricate the radiative cooler composed of thin film stacks deposited with electron beam evaporation (EBE) based on the optical constants of the oxides measured by our laboratory to make the optimization more accurate. The radiative coolers are comprehensively tested, and the solar spectrum reflectivity and atmospheric window emissivity in different angles are characterized. Results show that the developed radiative coolers have a satisfactory performance.

2 Method

2.1 Design

In the design of radiative coolers, one of the most important parameters is the complex refractive index $N = n - ik$, where the optical constants n and k represent the refractive index and extinction coefficient, respectively, and k is related to the absorption coefficient α by $\alpha = 4\pi k/\lambda$. As shown in Fig. 1, the optical constants n and k of various materials (SiO_2, HfO_2, TiO_2, Al_2O_3, and Ta_2O_5), which are widely used in radiative cooling due to their high absorption in the 8 to 13 μm waveband,[24,27,28] are plotted for comparison.

To improve the reflection in the solar spectrum, high-index and low-index materials in the solar spectrum are needed in the structure. SiO_2 with its refractive index of approximately near 1.44 in the solar spectrum and low absorption in the near-ultraviolet band is mostly used as the low-refractive-index material in the solar spectrum. Furthermore, SiO_2 also has a very high absorption in the 8 to 13 μm spectrum and its extinction coefficient k reaches a value of over 1.5 in the 9 to 10 μm waveband. As for high-index materials in the solar spectrum, both Ta_2O_5 and TiO_2 are considered. The refractive index of Ta_2O_5 is 2.1 and that of TiO_2 is 2.2 in the solar spectrum. Although TiO_2 has been used in many kinds of structures of photonic radiative coolers,[21] Ta_2O_5 is a comparatively better material in making radiative coolers. However, TiO_2 has a much higher absorption in the near-ultraviolet band than Ta_2O_5. Furthermore, the TiO generated during the TiO_2 coating process affects the experimental results. By contrast, Ta_2O_5 is a more stable material. In the solar spectrum, HfO_2 has low absorption in the near-ultraviolet band and

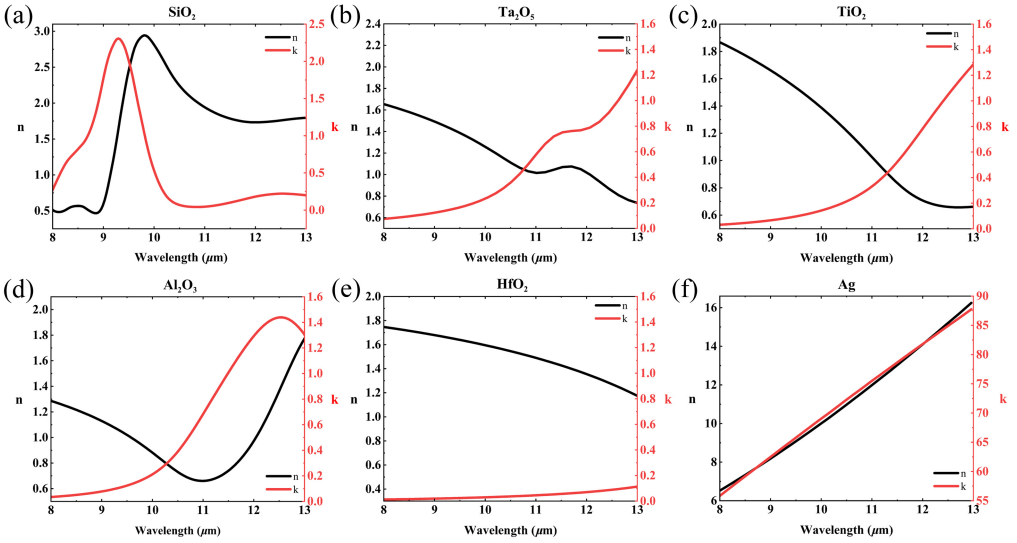

Fig. 1 Optical constants n and k of the materials in the 8 to 13 μm spectrum:[25,26] (a) optical constants of SiO_2, (b) optical constants of Ta_2O_5, (c) optical constants of TiO_2, (d) optical constants of Al_2O_3, (e) optical constants of HfO_2, and (f) optical constants of Ag.

can be a good material for optimizing reflection in the solar spectrum. However, its k is low in the 8 to 13 μm waveband. In addition, HfO_2 is a comparatively rare and expensive material. Al_2O_3 is a cheap and well-known oxide, and it has the highest absorption in the 11 to 13 μm spectrum among the aforementioned oxides. It is also used as the adhesion layer between the Ag layer and other oxide layers to enhance bonding, thus improving the reliability of the photonic radiative cooler. So we finally chose SiO_2, Ta_2O_5, and Al_2O_3 as the materials of oxide layers instead of HfO_2 and TiO_2.

The design began with calculating the optical properties of multilayered thin films, and the ultimate absorptivity, reflectivity, and transmissivity of a given wavelength were determined through iterative calculation by choosing the n, k, and d of each individual layer in the 8 to 13 μm waveband. The optical constants n and k of different materials vary in different ways in the 8 to 13 μm waveband, so we set some initial structures of different arrangements of layers, using commercial software (FilmWizard, Scientific Computing International, United States), which can optimize each layer with a given target.

Because SiO_2 is mostly used as a low-refractive-index oxide, we only tried different high-refractive-index oxides for the optimal design. Initially, we designed two types of radiative coolers composed of 10 alternating layers of SiO_2 (400 nm) and Ta_2O_5 (400 nm) or Al_2O_3 (400 nm) and Ag (200 nm) on the substrate; the structures were named structures 1 and 2, as shown in Fig. 2(a). To improve the reflection in the solar spectrum, we use 4 layers of alternating SiO_2 (50 nm) and Ta_2O_5 (50 nm) layers, and one layer of Ag (200 nm) at the bottom, as the reflection segment, which is responsible for increasing the reflection of incident light. On top of the reflection segment is the absorption segment with 12 layers of alternating SiO_2, Ta_2O_5, and Al_2O_3 layers in different orders; the structures were named structures 3 to 6, as shown in Fig. 2(b). During optimization, some single layers may be reduced to meet the demand for less thickness. The reason that our initial structures have so many layers and arrangements is to give the optimization more room to adjust.

Then we used the global optimization of the software and set 100% as the optimization target of absorption in the 8 to 13 μm waveband. After extensive numerical optimization, satisfactory results were obtained, as shown in Fig. 3. Taking structure 3 as an example, the average emissivity in the 8 to 13 μm spectrum of structure 3 slightly increased from 85.8% to 86.6%, but the total thickness of the structure significantly decreased from 3.8 to 2.58 μm. Similarly, the other five structures all showed a significant reduction in thickness and an obvious performance improvement. The results showed that a thin film using global optimization has a much better performance than simply changing the thickness and ratio of different materials, especially in reducing the thickness.

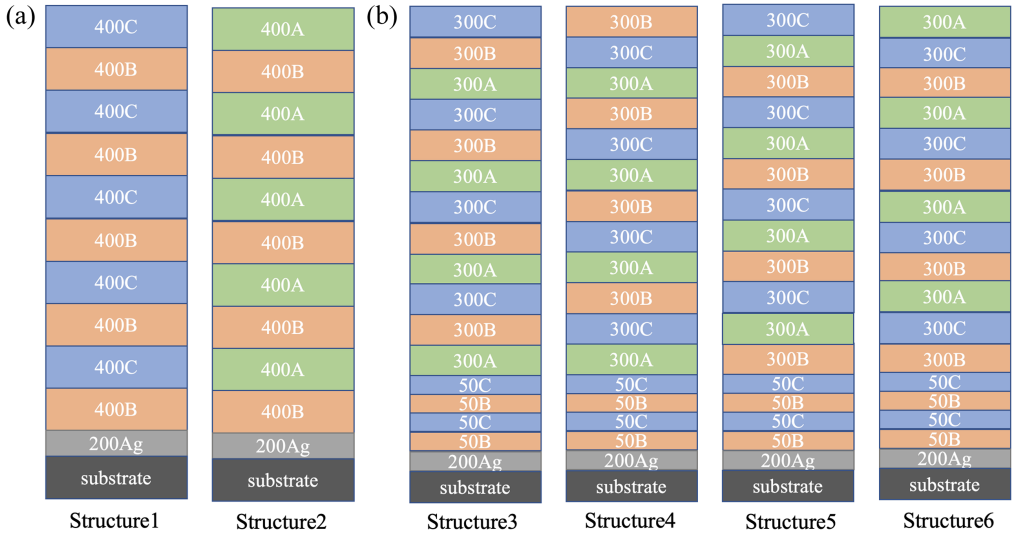

Fig. 2 (a) Initial structures of 10 layers of SiO_2 and Ta_2O_5 or Al_2O_3 and (b) initial structures of 10 layers of SiO_2, Ta_2O_5, and Al_2O_3 in different arrangements. (A: Al_2O_3, B: SiO_2, C: Ta_2O_5, unit: nm, and SUB: Si).

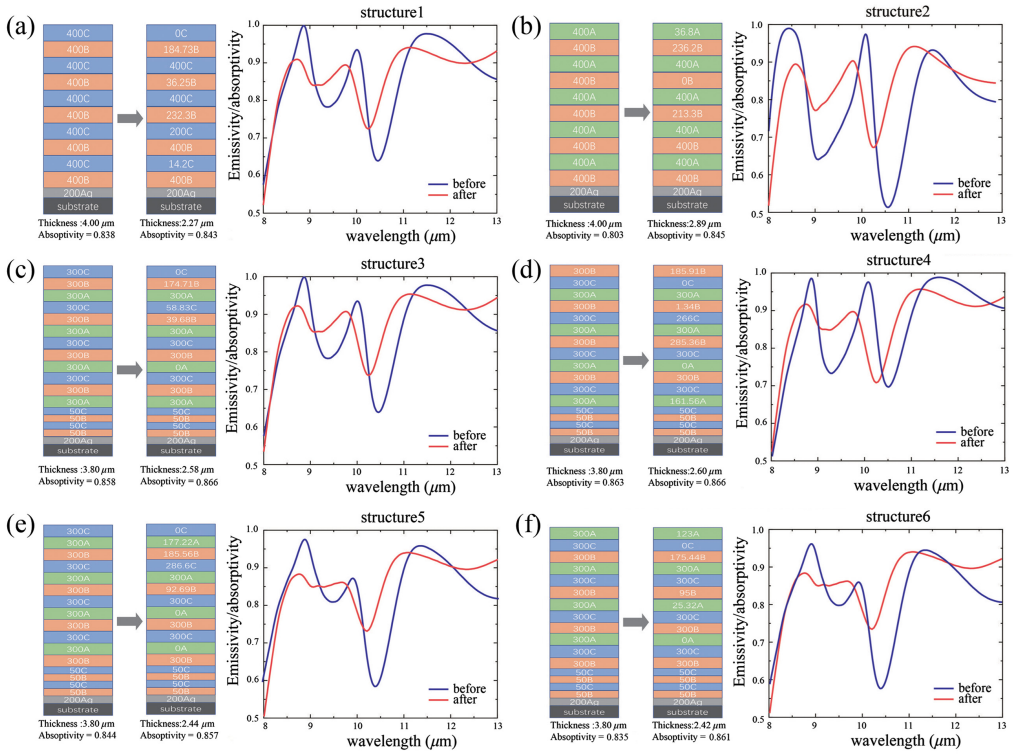

Fig. 3 (a)–(f) Schematic diagram and optical performance of the structures before and after the global optimization. (A: Al_2O_3, B: SiO_2, C: Ta_2O_5, unit: nm, and SUB: Si).

Al_2O_3 has a better adhesive force with the Ag layer than other oxides, so we use an Al_2O_3 layer as the bonding layer to improve the bonding force between the selective interference absorption layers and the metal reflector layer to prevent the film from cracking or delamination. For the same reason, to increase the adhesion between the metal reflector layer and the substrate, we chose to coat a very thin layer of Ni on the substrate before coating the Ag layer. The use of adhesion layers helps to improve the reliability. Finally, the main materials of our structures used

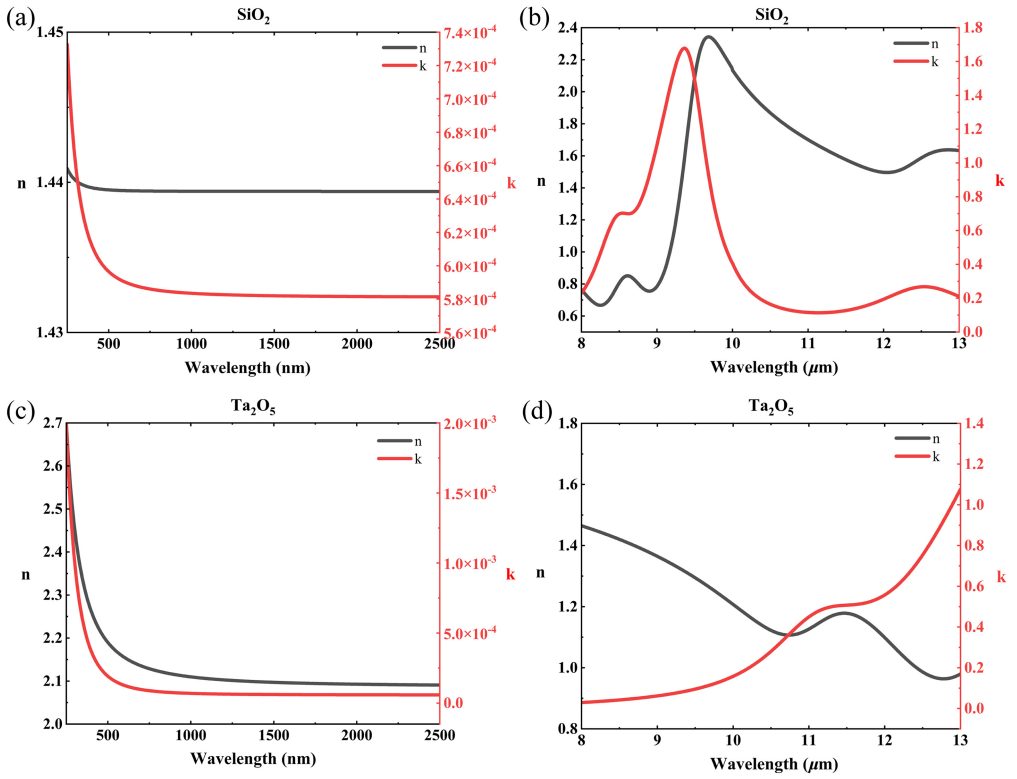

Fig. 4 Optical constants *n* and *k* of oxides in the solar spectrum and atmospheric window fitted by ellipsometry. (a) SiO_2 in the 250 to 2500 nm waveband. (b) SiO_2 in the 8 to 13 μm waveband. (c) Ta_2O_5 in the 250 to 2500 nm waveband. (d) Ta_2O_5 in the 8 to 13 μm waveband.

in the actual coating situation are SiO_2 and Ta_2O_5. The change of coating conditions such as coating methods, deposition temperature, and deposition rate will cause the change of film optical constants. Different from the conventional coating of oxides in EBE condition, with the combination of the Ag layer, the deposition temperature of the multilayer thin films is the room temperature without extra heat gain to avoid the Ag layer from oxidation.

To obtain the reliable optical constants of film materials in the EBE condition in this work, we measured the ellipsometry parameters psi and delta of SiO_2 and Ta_2O_5 films deposited at certain deposition temperatures and deposition rates in the 250 to 2500 nm and 8 to 13 μm spectra and fitted the optical constants in these spectra (Fig. 4). This makes our optimization more accurate and reliable than previous works. During the same process of design and optimization used before, we get two structures that meet the actual experimental conditions in our laboratory as the final structures (Tables 1 and 2). They both have a satisfactory performance of high reflectivity in the solar spectrum and high absorptivity/emissivity in the 8 to 13 μm spectrum.

Compared with prior works that simply changed the numbers of layers or thicknesses of each layer in optimizing the structures of the radiative coolers, this work has the following advantages.

1. Through accurate characterization of metal and dielectric films prepared under specific process conditions, such as certain deposition temperatures and deposition rates, etc., we obtained reliable optical constants of thin film source materials for deposition with EBE. With these specific optical constants, we optimized and fabricated the radiative coolers, which were thinner but had a higher radiative cooling performance.
2. Compared with the traditional radiative coolers, our work improved the mechanical properties of the thin-film device by adding an adhesion layer between the metal reflection layer and the selective interference absorption layer, which gave the thin film high environmental reliability and long life.

Table 1 Structural parameters of structure A.

Layer No.	Material	Thickness (nm)
10^{th}	SiO_2	186
9^{th}	Ta_2O_5	400
8^{th}	SiO_2	55
7^{th}	Ta_2O_5	400
6^{th}	SiO_2	86.6
5^{th}	Ta_2O_5	170
4^{th}	SiO_2	800
3^{rd}	Ta_2O_5	133
2^{nd}	Al_2O_3	50
1^{st}	Ag	200
Substrate	Si	/

Table 2 Structural parameters of structure B.

Layer No.	Material	Thickness (nm)
15^{th}	SiO_2	185
14^{th}	Ta_2O_5	300
13^{th}	SiO_2	35
12^{th}	Ta_2O_5	300
11^{th}	SiO_2	36
10^{th}	Ta_2O_5	300
9^{th}	SiO_2	228
8^{th}	Ta_2O_5	70
7^{th}	SiO_2	600
6^{th}	Ta_2O_5	19
5^{th}	SiO_2	25
4^{th}	Ta_2O_5	25
3^{rd}	SiO_2	34.5
2^{nd}	Al_2O_3	25
1^{st}	Ag	200
Substrate	Si	/

2.2 Fabrication

The thin-film radiative coolers were prepared by conventional EBE. When the chamber pressure reached 1×10^{-3} Pa, the ion source was turned on for bombardment cleaning of the substrate. The samples were not heated during the coating process. The Ag film was deposited by thermal evaporation, and the Al_2O_3, Ta_2O_5, and SiO_2 films were deposited by EBE. The deposition rate of Ag film was 1.0 nm/s. The deposition rates of the Al_2O_3, Ta_2O_5, and SiO_2 films were 0.8, 0.2, and 0.8 nm/s, respectively, and the deposition of the oxide dielectric films was assisted by the ion beam. The quartz crystal oscillator was used to monitor the deposition of the films to accurately control the thickness of each layer. Finally, the thin-film radiative coolers were fabricated by following the designed optimal structures.[29,30]

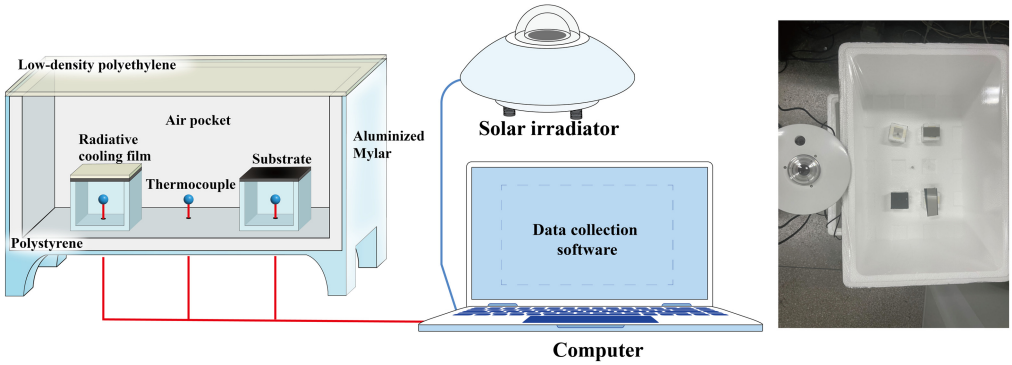

Fig. 5 Schematic and physical diagram of the temperature test structure.

2.3 Characterization

The test of the cooling effect was carried out under direct sunlight on a rooftop in Shanghai on June 10, 2023. We selected a large polystyrene box covered with aluminized mylar as a frame. Inside it were two small hollow polystyrene boxes covered by the radiative cooler and the uncoated substrate respectively, creating two sealed small air pockets. Thermocouples were used to record the temperature changes in different areas. One thermocouple went through the small hollow polystyrene box and was connected to the bottom of the radiative cooler, and one thermocouple went through another small hollow polystyrene box and was connected to the bottom of the uncoated substrate. Another thermocouple was used to record the temperature change inside the large polystyrene box. We calibrated all of the thermocouples before the experiment. A clear polyethylene film was wrapped around the whole structure, and the part where the probe is inserted was also sealed, creating a sealed big air pocket to prevent non-radiative heat exchange from air flow. The solar irradiometer was set next to the large polystyrene box to measure the solar illumination. All of the devices were connected to the laptop to record the data every second. The schematic and physical diagrams of the temperature test structure are shown in Fig. 5.

3 Results and Discussion

Figures 6 and 7 show the optical properties of the daytime photonic radiative cooler both in the solar spectrum and the 8 to 13 μm waveband. The solar spectrum includes three ranges: the ultraviolet (UV, 250 to 380 nm), visible (VIS, 380 to 750 nm), and near-infrared (NIR, 750-2500 nm). We set structure A, which has a better performance, as an example. Structure A has an average reflectivity of 0.981 in the NIR range, which accounts for 48.5% of the solar energy;

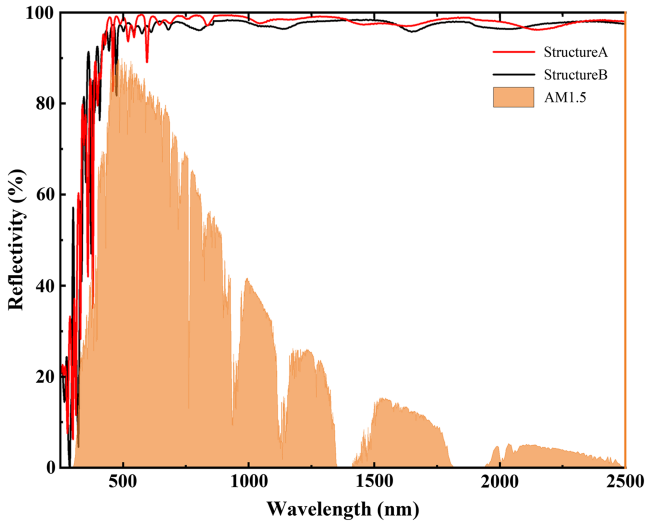

Fig. 6 Measured reflectivity in the solar spectrum of structure A and structure B.

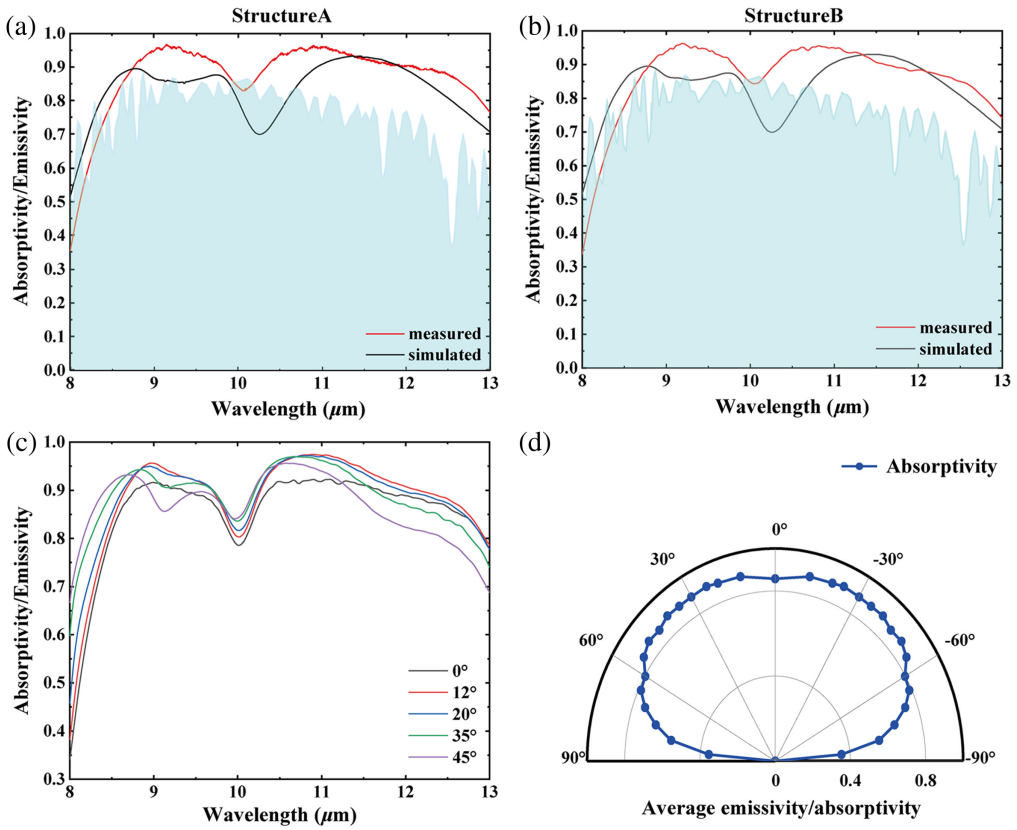

Fig. 7 Test effect of the radiative cooler: (a) measured emissivity in the solar spectrum of structure A, (b) measured emissivity in the solar spectrum of structure B, and (c) measured emissivity of photonic radiative cooler structure A between 8 and 13 at different angles of incidence. (d) Polar angle plot of the measured average emissivity of the photonic radiative cooler between 8 and 13 μm at different angles of incidence of structure A.

an average reflectivity of 0.962 in the VIS range, which accounts for 44.7% of the solar energy; and an average reflectivity of 0.421 in the ultraviolet range, which accounts for 6.8% of the solar energy. It has an average reflectivity of 0.963 between 250 and 2500 nm and reaches a reflectivity peak of 0.994 at 932 nm. Structure B has an average reflectivity of 0.975 in the NIR range, an average reflectivity of 0.959 in the VIS range, an average reflectivity of 0.437 in the ultraviolet range, and an average reflectivity of 0.956 between 250 to 2500 nm.

Structure A has a strong selective emissivity/absorptivity in the atmospheric window of 8 to 13 μm, achieving an average absorptivity of 0.876. Structure B also has a high absorption, with an average absorptivity of 0.872 in the 8 to 13 μm range. The measured emissivity of structure A between 8 and 13 μm at different angles of incidence is also shown in Fig. 7(d). The comparison of this work with previous multilayered photonic radiative coolers is given in Table 3, taking into account factors such as the solar reflectivity, atmospheric window absorption, and film thicknesses.

To characterize the daytime and nighttime cooling performance of the photonic radiative cooler, we measured the temperature of the cooler between 10:00 am and 1:30 pm as mentioned above and compared it with the temperature of the sealed air pocket and the uncoated substrate. Figure 8 shows the results of the radiative cooling effect of the developed coolers. The average solar intensity was 859.3 W/m^2 during the test. The sealed room was constantly exposed to the sun, causing its temperature to rise; the temperature of our radiative cooler also rose, but obviously more slowly than the uncoated substrate; and the temperature difference between them increased. After several hours, the temperature of the uncoated substrate reached a peak of 74.0°C, whereas the temperature of our radiative cooler was only 51.3°C. During the three hours of strongest sunlight, our radiative cooler achieved an average temperature reduction of 3.2°C compared with the ambient air, and the maximum temperature drop was 5.1°C at 10:39. Compared with the uncoated substrate, our radiative cooler achieved an average temperature reduction of 20.1°C.

Table 3 Performance of multilayer radiative cooling thin films.

Works	Structure	Thickness without metal and substrate (μm)	Average emissivity (8 to 13 μm)	Solar reflectivity
Raman et al.[19]	7 layers of 230 nm thick SiO_2, 485 nm thick HfO_2, 688 nm thick SiO_2, 13 nm thick HfO_2, 73 nm thick SiO_2, 34 nm thick HfO_2, and 54 nm thick SiO_2, with 200 nm thick Ag at the bottom.	1.577	0.67	0.97
Jeong et al.[21]	Eight alternating layers of 500 nm thick SiO_2 and 500 nm thick TiO_2, with 200 nm thick Ag at the bottom.	4	0.84	0.94
Kecebas et al.[20]	Nine alternating layers of TiO_2, SiO_2, Al_2O_3 each 300 nm thick and four alternating layers of TiO_2 and SiO_2 each 20 nm, with 50 nm thick Ag at the bottom.	2.78	0.78	Not mentioned
Ma et al.[22]	Seven layers of 257 nm thick SiO_2, 217 nm thick Si_3N_4, 421 nm thick SiO_2, 292 nm thick Si_3N_4, 418 nm thick SiO_2, 257 nm thick Si_3N_4, and 56 nm thick SiO_2, with 200 nm thick Ag at the bottom.	1.918	0.75	0.98
Chae et al.[31]	Three layers of 276 nm thick SiO_2, 312 nm thick Si_3N_4, and 1312 nm thick Al_2O_3, with 200 nm thick Ag at the bottom.	1.9	0.87	0.948
Kim et al.[23]	Eight layers of 180 nm thick Si_3N_4, 200 nm thick SiO_2, 1520 nm thick Al_2O_3, 570 nm thick SiO_2, 560 nm thick Si_3N_4, 1360 nm thick SiO_2, 1420 nm thick Si_3N_4, and 70 nm thick SiO_2, with 200 nm thick Ag at the bottom.	5.88	0.96	0.969
Xiao et al.[24]	18 alternating layers of three materials, SiN, SiO_2, and Ta_2O_5, on top of an Al mirror backreflector.	2.088	0.89	0.75
Structure A of this work	Shown in Table 1	2.28	0.876	0.963
Structure B of this work	Shown in Table 2	2.18	0.872	0.956

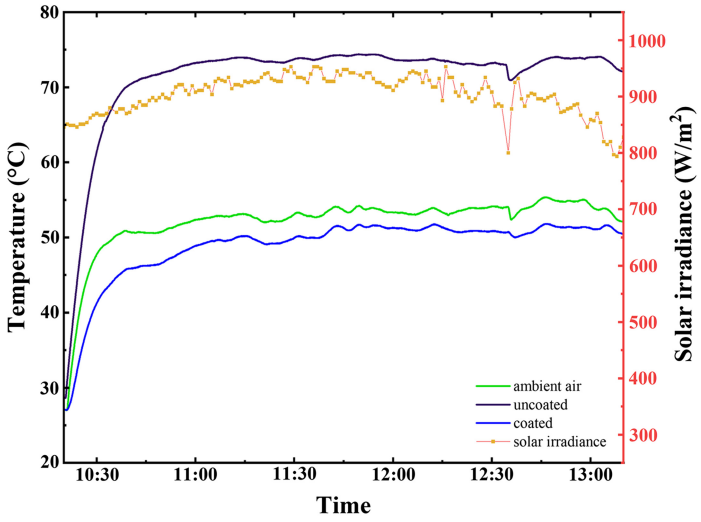

Fig. 8 Result of the outdoor temperature test from 10:00 am to 1:30 pm in Shanghai on June 10, 2023.

4 Conclusion

We developed a daytime radiative cooler composed of a substrate, a metal reflective layer, a dielectric bonding layer, and interference layers. All of the multilayer materials used in the radiative cooler were prepared in advance under specific process conditions, and their optical constants were accurately obtained for later design. The radiative coolers were designed and fabricated based on global optimization using the obtained optical constants. Finally, a radiative cooler with a thickness of 2.28 μm exhibited a reflectivity of 0.963 in the solar spectrum and an emissivity of 0.876 in the atmospheric window, and the performance was quite satisfactory in many respects compared with previous multilayered radiative coolers. The outdoor experiment showed that the radiative cooler was 22.3°C cooler than the uncoated substrate and 3.2°C cooler than the ambient temperature of the sealed room under direct sunlight with an average solar intensity of 859.3 W/m^2. This work indicates that designing the radiative cooler with the obtained data of multilayer thin film materials under specific process conditions and optimizing the thin film globally, rather than simply changing the number and thickness of layers, can significantly improve its performance.

Disclosures

The authors declare no conflicts of interest.

Code and Data Availability

Data underlying the results presented in this paper are not publicly available at this time but may be obtained from the authors upon reasonable request.

Funding

National Natural Science Foundation of China (Grant Nos. 62275053, 62275256, 61775042, and 11674062); National key Research and Development Program of China (Grant No. 2021YFB3701500); and Youth Innovation Promotion Association of the Chinese Academy of Sciences (Grant Nos. 2023248 and 2019241).

References

1. S. H. Fan, "Thermal photonics and energy applications," *Joule* **1**(2), 264–273 (2017).
2. W. M. Wang et al., "Performance assessment of a photonic radiative cooling system for office buildings," *Renew. Energy* **118**, 265–277 (2018).
3. W. Li and S. H. Fan, "Nanophotonic control of thermal radiation for energy applications [invited]," *Opt. Express* **26**(12), 15995–16021 (2018).
4. K. Panchabikesan, K. Vellaisamy, and V. Ramalingam, "Passive cooling potential in buildings under various climatic conditions in India," *Renew. Sust. Energy Rev.* **78**, 1236–1252 (2017).
5. E. Akerboom et al., "Passive radiative cooling of silicon solar modules with photonic silica microcylinders," *ACS Photonics* **9**(12), 3831–3840 (2022).
6. W. Li et al., "A comprehensive photonic approach for solar cell cooling," *ACS Photonics* **4**(4), 774–782 (2017).
7. S. Nizetic, E. Giama, and A. M. Papadopoulos, "Comprehensive analysis and general economic-environmental evaluation of cooling techniques for photovoltaic panels, part II: active cooling techniques," *Energy Convers. Manage.* **155**, 301–323 (2018).
8. Z. H. Li et al., "Fundamentals, materials, and applications for daytime radiative cooling," *Adv. Mater. Technol.* **5**(5), 1901007 (2020).
9. L. X. Zhu et al., "Radiative cooling of solar cells," *Optica* **1**(1), 32–38 (2014).
10. B. Zhao et al., "Spectrally selective approaches for passive cooling of solar cells: a review," *Appl. Energy* **262**, 114548 (2020).
11. K. C. Tang et al., "Temperature-adaptive radiative coating for all-season household thermal regulation," *Science* **374**(6574), 1504–1509 (2021).
12. S. C. Wang et al., "Scalable thermochromic smart windows with passive radiative cooling regulation," *Science* **374**(6574), 1501–1504 (2021).
13. L. Y. Zhou et al., "Radiative cooling for energy sustainability: materials, systems, and applications," *Phys. Rev. Mater.* **6**(9), 090201 (2022).
14. J. J. Greffet et al., "Coherent emission of light by thermal sources," *Nature* **416**(6876), 61–64 (2002).

15. A. R. Gentle and G. B. Smith, "Radiative heat pumping from the earth using surface phonon resonant nanoparticles," *Nano Lett.* **10**(2), 373–379 (2010).
16. E. A. Goldstein, A. P. Raman, and S. H. Fan, "Sub-ambient non-evaporative fluid cooling with the sky," *Nat. Energy* **2**(9), 17143 (2017).
17. S. Catalanotti et al., "Radiative cooling of selective surfaces," *Sol. Energy* **17**(2), 83–89 (1975).
18. J. L. Kou et al., "Daytime radiative cooling using near-black infrared emitters," *ACS Photonics* **4**(3), 626–630 (2017).
19. A. P. Raman et al., "Passive radiative cooling below ambient air temperature under direct sunlight," *Nature* **515**(7528), 540–544 (2014).
20. M. A. Kecebas et al., "Passive radiative cooling design with broadband optical thin-film filters," *J. Quantum Spectrosc. Radiat. Transf.* **198**, 179–186 (2017).
21. S. Y. Jeong et al., "Field investigation of a photonic multi-layered TiO_2 passive radiative cooler in sub-tropical climate," *Renew. Energy* **146**, 44–55 (2020).
22. H. C. Ma et al., "Multilayered Sio_2/Si_3N_4 photonic emitter to achieve high-performance all-day radiative cooling," *Sol. Energy Mater. Sol. C* **212**, 110584 (2020).
23. M. Kim et al., "Optimization and performance analysis of a multilayer structure for daytime radiative cooling," *J. Quantum Spectrosc. Radiat. Transf.* **260**, 107475 (2021).
24. W. Xiao et al., "Flexible thin film optical solar reflectors with Ta_2O_5-based multimaterial coatings for space radiative cooling," *APL Photonics* **8**, 090802 (2023).
25. N. F. Cunha et al., "Multilayer passive radiative selective cooling coating based on $Al/SiO_2/SiNx/SiO_2/TiO_2/SiO_2$ prepared by dc magnetron sputtering," *Thin Solid Films* **694**, 137736 (2020).
26. Z. M. Cheng et al., "Optical properties and cooling performance analyses of single-layer radiative cooling coating with mixture of TiO_2 particles and SiO_2 particles," *Sci. China Technol. Sci.* **64**(5), 1017–1029 (2021).
27. J. Kischkat et al., "Mid-infrared optical properties of thin films of aluminum oxide, titanium dioxide, silicon dioxide, aluminum nitride, and silicon nitride," *Appl. Opt.* **51**(28), 6789–6798 (2012).
28. T. J. Bright et al., "Infrared optical properties of amorphous and nanocrystalline Ta_2O_5 thin films," *J. Appl. Phys.* **114**(8), 083515 (2013).
29. B. J. Liu et al., "Effect of annealing temperature on structure and stress properties of Ta_2O_5/SiO_2 multilayer reflective coatings," *Acta Phys. Sin.* **68**(11), 114208 (2019).
30. X. H. Fu et al., "Different deposition technology affecting structure and performance of Si film," *Proc. SPIE* **6149**, 614937 (2006).
31. D. Chae et al., "Spectrally selective inorganic-based multilayer emitter for daytime radiative cooling," *ACS Appl. Mater. Interfaces* **12**(7), 8073–8081 (2020).

Yu-Shan Zhang is an ME candidate at Fudan University. He received his BE degree in the School of Optics and Photonics at Beijing Institute of Technology in 2021. His research focuses on daytime radiative cooling thin films and radiative cooling materials, especially oxides.

Bao-Jian Liu is a PhD candidate at Fudan University. He received his BE degree in inorganic nonmetallic material engineering from Shijiazhuang Tiedao University in 2011 and his ME degree in material engineering from Beihang University in 2014. His research interests focus on the characterization and fabrication of infrared optical coatings. He has authored and co-authored more than 10 technical journal papers and conference presentations.

Xiao-Jie Sun is a PhD candidate at Fudan University. She received her BE degree in the School of Information Science and Technology, Fudan University. Her research focuses on radiative cooling and phase-change materials.

Wei-Bo Duan is a professor at Shanghai Institute of Technical Physics. He received his PhD in physical electronics from Graduate University of Chinese Academy of Sciences. His research focuses on thin film coatings, especially infrared thin film devices and their applications in space remote sensing.

Yu-Ting Yang is a postgraduate student in the Department of Optical Science and Technology, School of Information Science and Engineering, Fudan University. Her research direction is the preparation and characterization of optical thin films.

De-Ming Yu is an engineer at Shanghai Institute of Technical Physics. He received his ME degree in material engineering from University of Shanghai for Science and Technology. His research focuses on infrared thin film coatings in space remote sensing.

Qing-Yuan Cai is a research professor at the Shanghai Institute of Technical Physics, Chinese Academy of Sciences. He received his PhD in optics from Fudan University, with a research interest in optical monitoring technologies for optical films. His research interest is in the development of optical film technology for aerospace optical remote sensing instruments.

Hao-Tian Zhang received his BS degree from the Department of Optical Science and Engineering, Fudan University, Shanghai, China, in 2019, where he is currently pursuing a PhD in the Department of Optical Science and Engineering. His research interests include nanometer-sized thin films, optical properties of solids, and optoelectronic instrumentation.

Lei Peng is currently a PhD student at the Department of Optical Science and Engineering, Fudan University, Shanghai. He received his MS degree in 2019. His research interests focus on optoelectronic properties of low-dimensional materials.

Rong-Jun Zhang received his PhD in solid state physics from Fudan University in 1999. He is a full professor in the School of Information Science and Engineering, Fudan University. During 2003 to 2004, he worked at Kiel University, Germany, as a visiting professor. During 2004 to 2006, he worked at the Max-Planck Institute for Microstructure Physics, Germany, as a Humboldt Research Fellow. His research interest mainly focuses on the optical properties of solids.

Yu-Xiang Zheng received his PhD from the Department of Physics, Fudan University, Shanghai, China, in 1996. He is a full professor in the Department of Optical Science and Engineering, Yiwu Research Institute, Fudan University. He has authored or coauthored more than 200 peer-reviewed journal articles and received more than ten patents. His research interests mainly include the optical properties of solids, advanced spectroscopic technology, and characterization of optical thin films.